PAPER

Check for updates

Iron-core/carbon-shell nanoparticles with intrinsic peroxidase activity: new platform for mimetic glucose detection†

N. S. Surgutskaya,[a] M. E. Trusova,[a] G. B. Slepchenko,[b] A. S. Minin,[c] A. G. Pershina,[ad] M. A. Uimin, [ID][c] A. E. Yermakov[c] and P. S. Postnikov [ID] *[e]

Artificial enzymatic mimics based on nanoparticles have become a powerful tool for the improvement of analytical performance in the detection of important bioactive compounds. For the first time the intrinsic peroxidase-like activity of Fe-core/carbon shell nanoparticles (Fe@C NPs) was studied. The catalytic process was described by a typical Michaelis–Menten curve for enzyme kinetics, and the results were comparable with those previously published. The high catalytic performance of the Fe@C NPs allows the development of a new simple procedure for glucose determination with a low detection limit of 0.21 μM. To our knowledge, this is the first study showing the ability to generate active oxygen species on the Fe@C surfaces. We suppose that our investigation will open up a new direction in medicinal applications using these promising materials.

Introduction

Since the year 2007, when the intrinsic peroxidase-like activity of Fe_3O_4 nanoparticles (NPs) was established, enzyme-mimicking sensors based on various nanoparticles have received enormous interest.[1] These NPs have significant advantages over natural enzymes.[2] For example, natural enzymes can be deactivated by protease or in the presence of alkali and strong acids.[3] Moreover, the enzymes require special conditions for storage.[4] In contrast, the NPs do not possess these disadvantages. The NPs demonstrate high activity, storage stability, operability and reproducibility of analytical results that makes them appealing for the design of sensors based on interactions with chromogenic peroxidase substrates.[5–7]

The most popular materials for sensor applications are Fe_3O_4 NPs, where the peroxidase-like activity is associated with the redox reaction of H_2O_2 with Fe^{2+}-ions on the nanoparticle surface.[8] However, the pristine Fe_3O_4 NPs have poor stability, relatively low magnetization and low solubility in acidic media. Therefore, the development of materials with intrinsic

peroxidase-like activity opened up a new direction in the preparation of new objects, substrates, and materials. These materials include metal oxide NPs, such as CuO,[9,10] Co_3O_4,[11] CeO_2,[12] V_2O_5-nanowires[13] and $CoFe_2O_4$,[14] metal sulfide NPs such as CuS[15] and FeS,[16] and noble metal NPs[17–19] with various content and morphologies. At this moment, the most promising materials for sensor technologies are carbon-based nanomaterials. Interestingly, the intrinsic peroxidase activity was established by active compounds immobilized on the carbon surface. For instance, carbon nanotubes loaded with Fe_3O_4 show high peroxidase activity ensured by the presence of metal oxide NPs. Hemin immobilized on graphene sheets is a prospect for the determination of single-nucleotide polymorphism. A hybrid material based on gold clusters and graphene oxide was synthesized, which demonstrated a surprising synergistic effect.[20] The resulting activities are much higher than those of isolated materials. Surprisingly, pure carbon materials also have an intrinsic peroxidase-like activity.[21–23] Thus, luminescent carbon nanoparticles[24] demonstrated unusually high activity towards H_2O_2 decomposition. Graphene oxide[23] shows a comparable effect explained by the presence of –COOH groups on the surface. The peroxidase-like activity of C_{60}-fullerene[22] can be explained in the same way. Previous researchers have observed a good correlation between the amount of COOH groups and the activity of the materials.

Recently, the focus of artificial enzyme design shifted towards a new generation of composites represented by magnetic materials coated by carbon.[25,26] The carbon layer on the NP surface improves the stability during storage,[27] decreases agglomeration and can serve as a platform for the covalent immobilization of organic functional groups.[28,29] Furthermore,

[a]Department of Biotechnology and Organic Chemistry, Tomsk Polytechnic University, Tomsk, 634050, Russia

[b]Department of Physical and Analytical Chemistry Tomsk Polytechnic University, Tomsk, 634050, Russia

[c]Institute of Metal Physics, Ural Branch, Russian Academy of Science, Yecaterinburg, 620990, Russia

[d]Siberian State Medical University, Tomsk, 634050, Russia

[e]Department of Technology of Organic Substrates and Polymer Materials, Tomsk Polytechnic University, Tomsk, 634050, Russia. E-mail: postnikov@tpu.ru

† Electronic supplementary information (ESI) available. See DOI: 10.1039/c7ay00598a

this type of NP demonstrates intrinsic activity comparable to the activity of their uncoated analogues, and their ability to generate active oxygen species means there is potential for anticancer therapeutics. However, the magnetization of Fe_3O_4-based NPs is relatively low, which results in difficult isolation and magnetic separation of nanoparticles from solution. Therefore, there is a need for a comprehensive study of other novel carbon-containing metal NPs with superior properties for peroxidase-like activity.

One of these materials is Fe-core/carbon shell NPs, which are the most promising materials for medicine and diagnostics.[30] These Fe@C NPs have sufficiently higher magnetization, monodispersity, and crystallinity. It was proven that Fe@C nanoparticles could be easily functionalized by organic functional groups *via* diazonium chemistry. The Fe@C nanoparticles exhibit intriguing catalytic activity. Previously we reported that the Fe@C NPs were able to activate H_2 dissociation with the formation of highly reactive species. The high catalytic activity is determined by the unique carbon shell which contains highly-energetic spaces and structural defects. These defects are able to significantly increase the peroxidase-like activity of the Fe@C NPs. Due to the mentioned benefits of the Fe@C NPs, we investigated the peroxidase-like activity in oxidative reactions with TMB and OPD and determined conditions for maximal activity. Based on the obtained results, we suggested and approbated a platform for a HRP mimetic sensor based on Fe@C NPs for the detection of glucose in water solutions.

Experimental

Materials and methods

Glucose oxidase (GO$_x$, 228 000 U g^{-1}), glucose, galactose, arabinose, lactose, maltose, 3,3′,5,5′-tetramethylbenzidine (TMB), *o*-phenylenediamine (OPD) and DMSO were supplied by Sigma-Aldrich. Serum and urine samples were provided by the Cardiology Research Institute (Tomsk, Russia). Banana juice, apple juice, pea juice, strawberry juice and pomegranate juice samples were purchased from local stores. A glucose assay kit was purchased from VECTOR-BEST.

Nanoparticle preparation

The Fe@C nanoparticles were prepared according to a published procedure[31] by the evaporation of overheated liquid drops of Fe in Ar flow containing butane.

Nanoparticle characterization

High-resolution transmission electron microscopy (HRTEM) investigation was carried out with a JEOL JEM 2100F microscope operated at 200 kV. Thermogravimetric analysis (TGA-MS) was carried out using a DSC-TG-MS 449PC Jupiter Netzsch (Netzsch GmbH, Germany) instrument coupled with a quadrupole mass spectrometer Netzsch 409 Aeolos (electron impact at 70 eV) in the temperature range of 25 to 1000 °C with linear heating (10 min^{-1}) of the sample in a corundum crucible under an air flow (40 mL min^{-1}). The main physical–chemical characteristics were totally characterized previously.[31–34]

Peroxidase-like activity of the Fe@C NPs

The procedure for the evaluation of peroxidase-like activity is based on a previously reported method for the determination of Fe_3O_4 activity.[8]

The peroxidase-like activity of the Fe@C nanoparticles was examined by adding 20 μL of the Fe@C solution (0.5 mg mL^{-1}) to 3 mL of 0.1 M NaOAc buffer (pH 3.6) containing 192 μL of H_2O_2 (30%) and 60 μL of TMB (10 mg mL^{-1} in DMSO) solutions.

The kinetic behaviour of Fe@C was studied by monitoring the absorbance in a time scan mode at 652 nm using a UV-Vis spectrophotometer Analytik Jena Specord 250 plus in 1 cm cuvettes. Kinetic investigations were carried out at 40 °C in 520 μL of NaOAc buffer (0.1 M, pH 3.6) with 20 μL of the Fe@C solution (0.5 mg mL^{-1}). Kinetic measurements with 30% H_2O_2 as a substrate were carried out with a constant volume of TMB solution (10 μL, 10 mg mL^{-1} in DMSO) and different amounts of 30% H_2O_2 (0, 2, 4, 6, 8, 16, 32 and 48 μL). Kinetic analysis with TMB as a substrate was carried out with 32 μL of H_2O_2 and different amounts of TMB solution (0.5, 1, 2, 4, 6, 8, 10 and 12 μL). All measurements were repeated three times and showed high reproducibility over three repeated experiments.

The initial velocities were calculated using the molar extinction coefficient of oxidized TMB 39 000 M^{-1} cm^{-1}. The Michaelis constant and maximal reaction velocities for TMB and H_2O_2 as substrates were calculated using Lineweaver–Burk plots of the double reciprocal of the Michaelis–Menten equation

$$\frac{1}{V} = \frac{K_m}{V_{max}} \frac{1}{[S]} + \frac{1}{V_{max}},$$

where V is the initial velocity, K_m is the Michaelis constant, $[S]$ is substrate concentration and V_{max} is the maximal reaction velocity.

Glucose detection with the Fe@C NPs

Glucose detection was carried out in the three following steps.[21,22] First, 50 μL of GO$_x$ (1 mg mL^{-1}) and 50 μL of glucose with different molar concentrations were diluted in 150 μL of PBS buffer solution (10 mM, pH 7.0) and incubated at 37 °C for 30 min. After that, 50 μL of the above glucose reaction solutions, 10 μL of TMB (10 mg mL^{-1} in DMSO), and 20 μL of the Fe@C solution (0.5 mg mL^{-1}) were added to 520 μL of NaOAc buffer solution (0.1 M, pH 3.6). The resulting reaction mixtures were incubated at 40 °C for 1 h. Then the absorbance was measured at 652 nm according to the standard procedures for the standard curve construction.

Biological fluids, serum and urine samples for the glucose detection were centrifuged at 4000 rpm for 5 min and the supernatants were diluted 5 and 10 times for the serum and 20 times for the urine samples. The diluted samples (50 μL) were analyzed according to procedure described above.

For the detection of glucose in juice, each sample (banana, apple, pea, strawberry and pomegranate juice) was centrifuged at 10 000 rpm for 5 min and the supernatants were diluted 100 fold. The diluted samples (50 μL) were added to the solution of 50 μL of GO$_x$ and 150 μL of PBS buffer and incubated at 37 °C for

30 min. Then, 50 µL of each reaction solution, 10 µL of TMB (10 mg mL^{-1} in DMSO), and 20 µL of the Fe@C solution (0.5 mg mL^{-1}) were added to 520 µL of 0.1 M NaOAc buffer (pH 3.6) and the resulting mixtures were incubated at 40 °C for 1 h. The glucose concentrations in each sample were measured at 652 nm according to the standard glucose curve.

An enzymatic glucose assay kit was used to confirm the reliability of the method (explained in the ESI†).

Results and discussion

Previously we described a convenient method for the preparation of Fe@C and Ni@C nanocomposites *via* slow evaporation of melted metal drops in a stream of Ar containing hydrocarbons.[34] Fe@C NPs draw a lot of attention due to their biocompatibility, stability, and narrow size distribution.

The prepared Fe@C nanoparticles are nearly-spherical nanoobjects with an average size of about 10 nm (Fig. 1). The phase composition, determined by XRD measurements, is represented by three main components: α-Fe, Fe$_3$C, and carbon. The obtained nanopowders have high magnetization: about 110 emu g^{-1}.[34] The detailed structure was evaluated previously.[31–34]

Determination of the peroxidase-like activity of Fe@C was carried out using a well-proven method for Fe$_3$O$_4$ NPs.[8] The procedure consists of an interaction between H$_2$O$_2$ and Fe@C followed by oxidation of chromogenic peroxidase substrates, such as 3,3′,5,5′-tetramethylbenzidine (TMB) and *o*-phenylenediamine (OPD) (Fig. 2). The resulting product of TMB and OPD oxidation has a maximum absorbance at 652 and 450 nm, respectively. The significant shifts of absorbance make these reactions suitable for direct colorimetric determination.

The catalytic activity of metal NPs depends on pH and temperature.[1] We carried out experiments for the evaluation of the pH and temperature influence on the NP catalytic activity. For these purposes, we measured the peroxidase activity in the pH range of 1–8 and temperature range of 25–90 °C. 0.1 M citrate, NaOAc, PBS and borax buffers were used as reaction media for the pH-dependent measurement. For the
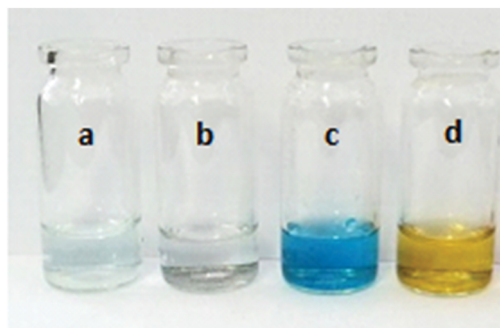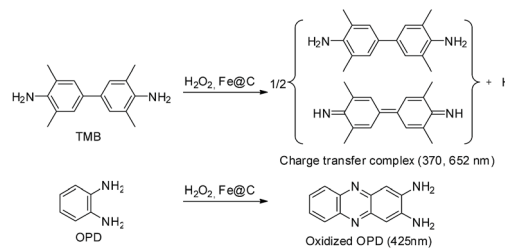

Fig. 2 The scheme for the Fe@C catalytic oxidation of various peroxidase substrates. The images show TMB oxidation by H$_2$O$_2$ with and without Fe@C nanoparticles ((a) H$_2$O$_2$ and TMB; (b) Fe@C NPs and TMB; (c) H$_2$O$_2$, TMB and Fe@C NPs; (d) the formation of oxidized OPD in the presence of H$_2$O$_2$ and Fe@C).

measurement of the temperature–activity relationship, we incubated the reaction mixtures for 15 min at all required temperatures before carrying out the catalytic activity tests. We found that the optimal temperature range for the highest activity of the Fe@C NPs is 30–40 °C while the optimal pH range is 3.6–4.4 (Fig. S1a and b†), which are similar with the optimal enzyme pH and temperature ranges published previously.[1] The optimal Fe@C concentration was determined using the optimal pH and temperature parameters and should not be lower than 16 µg mL^{-1} (Fig. S1c†).

The most important property of carbon and carbon-coated nanomaterials is the improved stability of their catalytic properties. We evaluated the stability of the peroxidase-like activity of the Fe@C nanoparticles after incubation in solutions with the pH range of 1 to 8 and temperature range of 30 to 90 °C (Fig. S2†). The obtained results demonstrated the great reproducibility of the intrinsic enzymatic activity of the Fe@C NPs.

Kinetic investigations of TMB oxidation were carried out at optimal temperature, pH and nanoparticle concentration and with different concentrations of H$_2$O$_2$ and TMB according to the enzyme kinetic theory and assays. The initial velocities were calculated from the values of the slopes and the extinction coefficient 39 000 M^{-1} cm^{-1} of oxidized TMB as stated previously.[8] The obtained kinetic curves (Fig. 3a and b) have an excellent agreement with the Michaelis–Menten equation for enzyme kinetics. Moreover, the shape and basic parameters of the curve are similar to those in published investigations of the intrinsic peroxidase-like activity of other nanomaterials.[1,8,22] The main kinetic parameters, such as the Michaelis constant (K_m) and maximum reaction velocities (V_{max}), were calculated using the transformation of the curves to a linear form (Fig. 3c
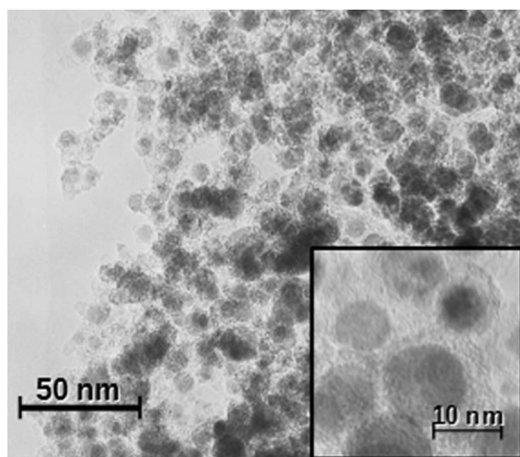

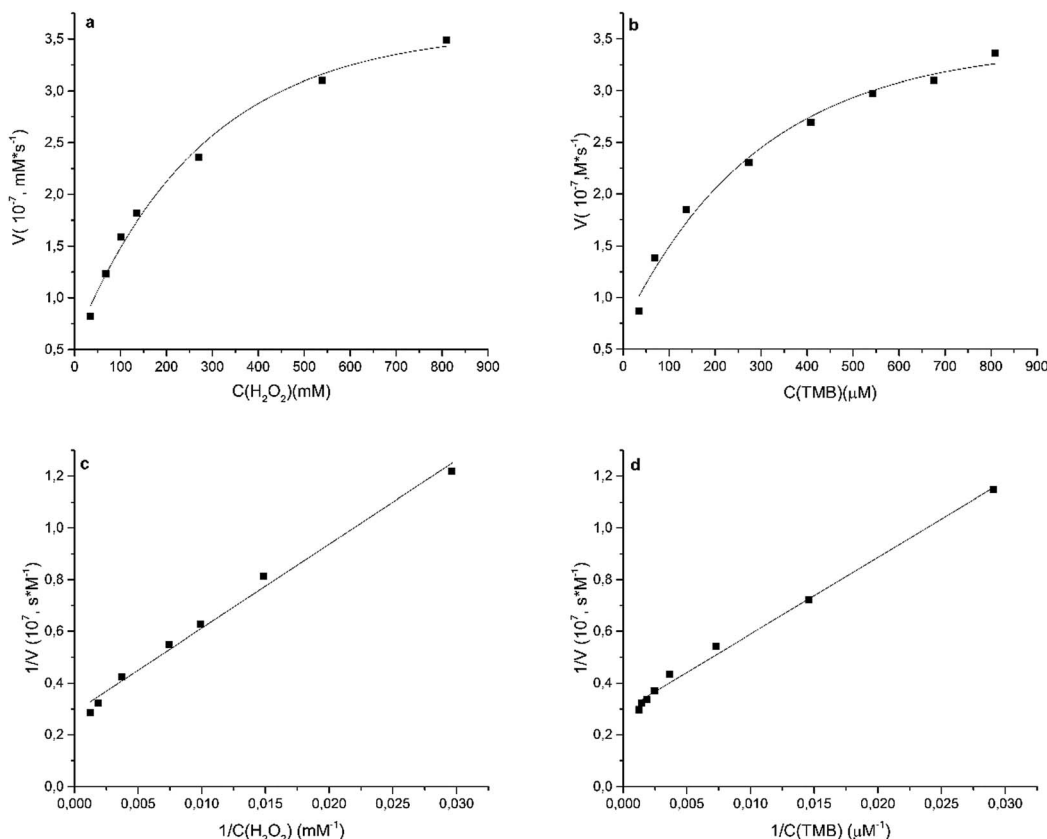Fig. 1 TEM image of the Fe@C nanoparticles.

Fig. 3 Kinetic curves of the TMB oxidation (a and b) in direct and (c and d) in double reciprocal coordinates in the presence of the Fe@C nanoparticles. (a and c) The TMB concentration was constant and the H_2O_2 concentration was varied and (b and d) the TMB concentration was varied.

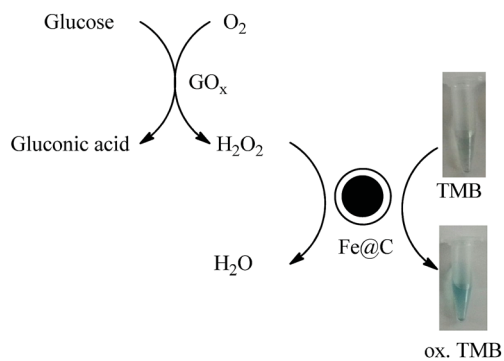Fig. 4 Schematic illustration of colorimetric glucose detection using glucose oxidase (GO_x) and Fe@C-catalyzed reactions.
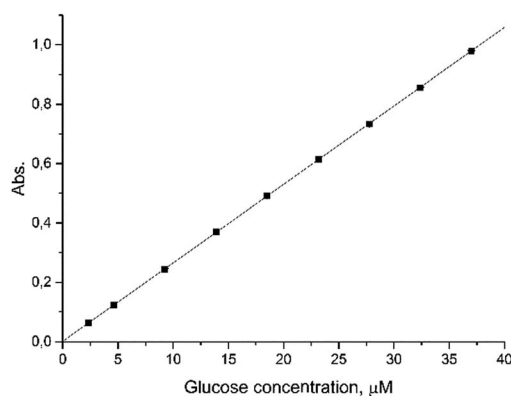

Fig. 5 The response curve for glucose detection with the Fe@C nanoparticles and TMB as the chromogenic substrate. The error bars represent the standard deviation for three measurements.

and d) according to the Lineweaver–Burk plot (Table S1†). The estimated parameters were comparable with HRP and another peroxidase-like nanomaterial.[8] The obtained results (Table S1†) showed that the nanoparticles have a 4 times higher reaction rate than the appropriate enzyme. The apparent K_m value of the Fe@C nanoparticles was lower than that of the enzyme, suggesting that the Fe@C NPs have a higher affinity for TMB than HRP. At the same time, the K_m value of Fe@C with H_2O_2 as the substrate was notably higher than for HRP. This indicates that

a higher concentration of H_2O_2 is required for maximal activity of the NPs. Comparison with other nanomaterials (Table S1†) revealed that the Fe@C NPs have a middle position between iron oxide nanomaterials and carbon-based nanoparticles. Thus, the K_m value of the Fe@C NPs with H_2O_2 is more than 1.5 and 3 times lower than that of the Fe_3O_4 nanoparticles and PBMNPs, respectively, which indicates the higher affinity of
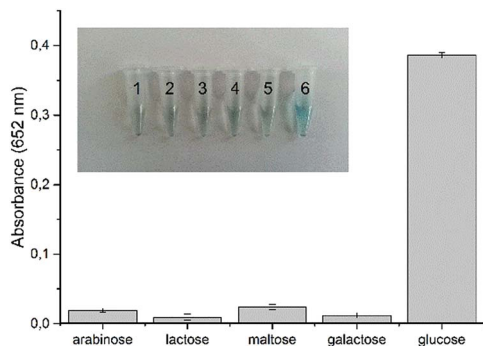
Fig. 6 Selectivity of glucose detection. Blank sample (1), arabinose (2), lactose (3), maltose (4), galactose (5) and glucose (6), error bars represent the standard deviation for three measurements.

Fe@C NPs.[1,8] The same parameter for the Fe@C NPs is higher than for C_{60}-carboxyfullerenes and composite Fe_3O_4@C nanoparticles. However, the mentioned difference can be explained by the presence of carboxylic groups on the surface of C_{60}-carboxyfullerenes and composite Fe_3O_4@C nanoparticles.[22,25] Unfortunately, calculation of the catalytic constant was complicated because the nature of the active centres is not clearly determined. Our previous study showed that the catalytic activity of Fe@C NPs in the reaction of H_2 dissociation is connected with Stone–Wales defects of the carbon layers.[32,33] The peroxidase-like activity can be determined by the presence of Fe_3C under the carbon layers. We proposed that both factors (the Stone–Wales defects and the presence of Fe_3C) affected the intrinsic mimic activity of this material.

Glucose detection with Fe@C

One of the most important applications of artificial mimicking NPs is the detection of key biologically active products, such as glucose.[6,10,16] We proposed that the advantages of the Fe@C NPs would be useful for colorimetric determination of glucose. The convenient procedure includes two steps: the oxidation of

glucose by GO_x followed by the formation of H_2O_2 and gluconic acid, and the reaction of H_2O_2 with the Fe@C NPs (Fig. 4). As a result, TMB is readily oxidized, and the concentration of the product can be simply measured using UV-Vis spectroscopy.

Optimisation of the first-step parameters includes the determination of the GO_x concentration and incubation time in order to improve the efficiency of the detection system. As shown in Fig. S3 and S4 in the ESI,† the optimal GO_x concentration is 0.2 mg mL^{-1} and the incubation time is equal to or more than 20 min. We also estimated the optimal reaction time of the Fe@C NPs with the activated glucose solution as being 1 h (Fig. S5†). The optimal conditions have been used for the glucose determination.

The experimental study of the Fe@C-assisted determination of glucose demonstrated satisfactory results. All measurements were carried out at optimal pH and temperature in order to simplify the experimental procedure. We found that the absorbance at 652 nm was proportionally increased in the glucose concentration range of 2.06–37 μM (Fig. 5) according to the equation $A_{652 \text{ nm}} = 0.0265x$ ($R = 0.9985$) with a good detection limit of 0.21 μM (3σ/slope; where σ – standard deviation of the regression).

Surprisingly, the detection limit was quite low (Table S2†). For instance, the detection limit of glucose by Fe_3O_4 NPs coated by carbon was 2 μM.[26] The DNA–nanoceria conjugates[7] and carbon NPs[24] allow the detection of only 8.9 and 20 μM glucose respectively. The obtained results can improve the analytic performance of glucose determination using artificial mimics.

In order to evaluate the selectivity of the Fe@C NPs toward saccharides we carried out model experiments with galactose, arabinose, lactose, and maltose. For the activity screening we chose the same concentrations of saccharides and glucose (1.35 mM). All measurements were performed under the same conditions, according to the standard procedure for glucose detection. The control experiment showed a high selectivity of the method toward glucose. Samples containing another type of saccharide show the same results as the blank solution (Fig. 6). Thus, we proved the high selectivity of Fe@C toward glucose.

Table 1 Determination of glucose in serum and urine samples

Sample no.	Dilution	Result in diluted samples (μM)	Added	Recovery (%)	RSD ($n = 5$) %	Experimental result (mM)	Glucose assay kit (mM)
Serum samples							
1	600	23.55			0.58	14.13 ± 0.10	14.34 ± 0.42
2	300	15.69			0.54	4.71 ± 0.03	4.80 ± 0.34
3	300	13.59	5	97.4	1.28	4.07 ± 0.07	3.83 ± 0.31
			10	95.5			
			15	101.7			
			20	96.7			
4	300	29.31			0.52	8.79 ± 0.06	8.61 ± 0.41
5	600	23.36			0.81	14.02 ± 0.14	14.21 ± 0.28
Urine samples							
1	30.09	1200			0.75	36.11 ± 0.34	36.97 ± 0.38
			5	96.4	1.16	25.03 ± 0.36	24.97 ± 0.58
2	20.86		10	95.5			
			15	96.6			

The observed effects allowed the development of a procedure for the direct determination of glucose in food samples.

Determination of glucose in food samples using Fe@C

The applicability of the Fe@C NPs as a peroxidase mimic was investigated through the determination of glucose in biological fluids and juice samples. We tested all of the samples using the Fe@C NPs and an enzymatic glucose assay kit as a reference method (Tables 1 and S2†). We found that the proposed system is extremely sensitive: glucose detection was carried out in serum samples with dilutions of up to 300, and urine samples with up to 1200 and juice samples with up to 6000 fold dilutions.

The determined glucose concentration in different serum and urine samples varied from 4.07 mM to 30.09 mM (Table 1). Moreover, the proposed method has high reliability and reproducibility: the relative standard deviation (RSD) for 5 samples was around 0.52–1.28% and recovery after the addition of the standard glucose solutions to the original samples was around 95.5–101.7%. The same results were obtained with the juice samples (Table S3†), where the recovery falls in the range of 94.7–98.0% and the RSD is not above 5%.

Moreover, the concentrations of glucose determined using the Fe@C NPs are similar with the results of the experiment based on the enzymatic glucose assay kit. Taking into account the stability of Fe@C during storage and repeatability of the results, we developed a good alternative approach to the classic enzymatic method.

Consequently, colorimetric sensing with the Fe@C nanoparticles is applicable for glucose detection in biological fluids and liquid food products with high selectivity and sensitivity.

Conclusions

In summary, the Fe@C nanoparticles showed high catalytic activity as peroxidase mimics in the oxidation of peroxidase substrates in the presence of H_2O_2. The catalytic process was described by a typical Michaelis–Menten curve for enzyme kinetics. Furthermore, the prepared nanoparticles can be used as HRP mimetic sensors for the colorimetric detection of glucose in water solutions in the concentration range of 2.31 μM to 37 μM with a low detection limit of 0.21 μM. The described method is applicable for glucose detection in diluted water solutions of biological fluids and liquid food products (juices) and is characterized by its simplicity of performance and reproducibility of results.

Acknowledgements

References

1 L. Gao, J. Zhuang, L. Nie, J. Zhang, Y. Zhang, N. Gu, T. Wang, J. Feng, D. Yang, S. Perrett and X. Yan, *Nat. Nanotechnol.*, 2007, **2**, 577–583.

2 Y. Lin, J. Ren and X. Qu, *Acc. Chem. Res.*, 2014, **47**, 1097–1105.

3 J. Xie, X. Zhang, H. Wang, H. Zheng and Y. Huang, *Trends Anal. Chem.*, 2012, **39**, 114–129.

4 P. V. Iyer and L. Ananthanarayan, *Process Biochem.*, 2008, **43**, 1019–1032.

5 S. Dutta, C. Ray, S. Mallick, S. Sarkar, R. Sahoo, Y. Negishi and T. Pal, *J. Phys. Chem. C*, 2015, **119**, 23790–23800.

6 L. Han, C. Li, T. Zhang, Q. Lang and A. Liu, *ACS Appl. Mater. Interfaces*, 2015, **7**, 14463–14470.

7 B. Liu, Z. Sun, P. J. Huang and J. Liu, *J. Am. Chem. Soc.*, 2015, **137**, 1290–1295.

8 X. Zhang, S. Gong, Y. Zhang, T. Yang, C. Wang and N. Gu, *J. Mater. Chem.*, 2010, **20**, 5110–5116.

9 W. Chen, J. Chen, A.-L. Liu, L.-M. Wang, G.-W. Li and X.-H. Lin, *ChemCatChem*, 2011, **3**, 1151–1154.

10 W. Chen, J. Chen, Y. Feng, L. Hong, Q.-Y. Chen, L.-F. Wu, X.-H. Lin and X.-H. Xia, *Analyst*, 2012, **137**, 1706–1712.

11 H. Jia, D. Yang, X. Han, J. Cai, H. Liu and W. He, *Nanoscale*, 2016, **8**, 5938–5945.

12 H. Zhao, Y. Dong, P. Jiang, G. Wang and J. Zhang, *ACS Appl. Mater. Interfaces*, 2015, **7**, 6451–6461.

13 R. André, F. Natálio, M. Humanes, J. Leppin, K. Heinz, R. Wever, H.-C. Schröder, W. E. G. Müller and W. Tremel, *Adv. Funct. Mater.*, 2010, **21**, 501–509.

14 K. Zhang, W. Zuo, Z. Wang, J. Liu, T. Li, B. Wang and Z. Yang, *RSC Adv.*, 2015, **5**, 10632–10640.

15 Q. W. Shu, C. M. Li, P. F. Gao, M. X. Gao and C. Z. Huang, *RSC Adv.*, 2015, **5**, 17458–17465.

16 C. Ding, Y. Yan, D. Xiang, C. Zhang and Y. Xian, *Microchim. Acta*, 2016, **183**, 625–631.

17 S. Wang, W. Chen, A.-L. Liu, L. Hong, H.-H. Deng and X.-H. Lin, *ChemPhysChem*, 2012, **13**, 1199–1204.

18 C. Zheng, W. Ke, T. Yin and X. An, *RSC Adv.*, 2016, **6**, 35280–35286.

19 J. Lia, W. Liu, X. Wu and X. Gao, *Biomaterials*, 2015, **48**, 37–44.

20 Y. Tao, Y. Lin, Z. Huang, J. Ren and X. Qu, *Adv. Mater.*, 2013, **25**, 2594–2599.

21 A.-X. Zheng, Z.-X. Cong, J.-R. Wang, J. Li, H.-H. Yang and G.-N. Chen, *Biosens. Bioelectron.*, 2013, **49**, 519–524.

22 R. Li, M. Zhen, M. Guan, D. Chen, G. Zhang, J. Ge, P. Gong, C. Wang and C. Shu, *Biosens. Bioelectron.*, 2013, **47**, 502–507.

23 Y. Song, K. Qu, C. Zhao, J. Ren and X. Qu, *Adv. Mater.*, 2010, **22**, 2206–2210.

24 X. Wang, K. Qu, B. Xu, J. Ren and X. Qu, *Nano Res.*, 2011, **4**, 908–920.

25 Q. An, C. Sun, D. Li, K. Xu, J. Guo and C. Wang, *ACS Appl. Mater. Interfaces*, 2013, **5**, 13248–13257.

26 Q. Li, G. Tang, X. Xiong, Y. Cao, L. Chen, F. Xu and H. Tan, *Sens. Actuators, B*, 2015, **215**, 86–92.

27 I. K. Herrmann, R. N. Grass, D. Mazunin and W. J. Stark, *Chem. Mater.*, 2009, **21**, 3275–3281.

28 R. N. Grass, E. K. Athanassiou and W. J. Stark, *Angew. Chem., Int. Ed.*, 2007, **46**, 4909–4912.

29 P. S. Postnikov, M. E. Trusova, T. A. Fedushchak, M. A. Uimin, A. E. Ermakov and V. D. Filimonov, *Nanotechnol. Russ.*, 2010, **7–8**, 15–16.

30 I. K. Herrmann, B. Beck-Schimmer, C. M. Schumacher, S. Gschwind, A. Kaech, U. Ziegler, P.-A. Clavien, D. Günther, W. J. Stark, R. Graf and A. A. Schlegel, *Nanomedicine*, 2016, **11**, 783–796.

31 V. R. Galakhov, A. S. Shkvarin, A. S. Semenova, M. A. Uimin, A. A. Mysik, N. N. Shchegoleva, A. Ye. Yermakov and E. Z. Kurmaev, *J. Phys. Chem.*, 2010, **114**, 22413–22416.

32 A. V. Erokhin, E. S. Lokteva, A. Y. Yermakov, D. W. Boukhvalov, K. I. Maslakov, E. V. Golubina and M. A. Uimin, *Carbon*, 2014, **74**, 291–301.

33 V. R. Galakhov, S. N. Shamin, E. M. Mironova, M. A. Uimin, A. Y. Yermakov and D. W. Boukhvalov, *JETP Lett.*, 2012, **96**, 710–713.

34 V. A. Tsurin, A. Y. Yermakov, M. A. Uimin, A. A. Mysik, N. N. Shchegoleva, V. S. Gaviko and V. V. Maikov, *Phys. Solid State*, 2014, **56**, 287–300.